15.7 A 144GHz 0.76cm-Resolution Sub-Carrier SAR Phase Radar for 3D Imaging in 65nm CMOS

Adrian Tang[1], G. Virbila[1], D. Murphy[1], F. Hsiao[1], Y.H. Wang[1], Q. J. Gu[2], Z. Xu[3], Y. Wu[4], M. Zhu[1], Mau-Chung Frank Chang[1]

[1]University of California, Los Angeles, Los Angeles, CA
[2]University of Florida, Gainsville, FL
[3]HRL, Malibu, CA
[4]Northrop Grumman Aerospace Systems, Los Angeles, CA

Millimeter-Wave-based radar has gained attention in recent years for automotive and object detection applications [1]. Several new applications are also emerging which employ mm-Wave radar techniques to construct short range mm-Wave 3D imaging systems for security screening and biomedical applications [2]. At present, these types of 3D mm-Wave imagers have only been demonstrated in III-V technology, as CMOS-based radar suffers several range and resolution limitations due to limited output power and linearity.

Most CMOS mm-Wave radar systems used in automotive applications are based on Frequency-Modulated Continuous-Wave (FMCW) ranging techniques in which the carrier is swept to produce a frequency offset at the receiver output proportional to the round-trip distance between the radar and target [3]. While FMCW is an excellent approach for accurate ranging, its implementation becomes particularly difficult at high frequencies as the resolution is heavily dependent on sweep linearity and the high RF front-end performance required to support the wideband swept carrier. For 3D mm-Wave imaging applications, this high operating frequency is indispensable as the attainable spatial (XY) resolution is fundamentally limited by the wavelength of the imaging system. Higher frequency also helps relax focusing lens requirements, as the optical diffraction limit is set by the ratio of the radar wavelength over the lens aperture size.

Phase-based radar is an alternative approach to ranging, and directly measures the round-trip time by estimating the phase delay of the carrier. Its unique advantages include the fact that that the carrier does not need to sweep across a wide frequency range, relaxing RF front-end bandwidth and linearity requirements. Its resolution is limited only by the system noise, allowing very high resolution to be achieved if long integration periods are used. Provided the target is a slow motion object (<10m/sec) for security screening, an integration time of 2μs would only produce 0.02mm of distance inaccuracy and 0.016mm of inaccuracy associated with the Doppler shift. The only issue that limits the use of phase-based radar is its intrinsic range ambiguity as the target travels beyond 1 wavelength of the carrier. To alleviate this ambiguity we propose sub-carrier successive-approximation radar (SAR) which operates as follows:

As directly resolving the phase at the carrier frequency of 144GHz is quite difficult, we instead propose to conduct successive ranging measurements at increasing IF frequencies within 1 to 400 MHz to eliminate the range ambiguity. In this demonstrated 2-step successive-approximation system shown in Fig 15.7.1, a coarse scan is first performed at an IF of 189MHz and a 50%-of-wavelength decision is made. Every pixel depth value in the coarse scan is either 0 or half of the wavelength of 189MHz. Then a fine scan is performed at 378MHz to provide the higher resolution. Finally, the coarse and fine scanning results are added to produce a final 3D image. These two frequencies (189/378MHz) were chosen specifically to emphasize the difference between coarse and fine capture for the scene content presented in this paper. The final combined capture would be similar regardless of the coarse and fine frequency selection, with the depth resolution determined by the fine frequency selection only.

As seen in Fig. 15.7.1 the proposed radar system consists of 3 separate chips: transmitter, receiver and phase estimator. The transmitter (TX) and receiver (RX) chips contain a 48GHz mm-Wave synthesizer cascaded with a nonlinear amplifier to generate a large 3rd-order harmonic and provide a subharmonic injection locking [4] to a 144GHz oscillator used for the LO. The mm-Wave synthesizer is a derivative of the one presented in [5]. Both TX and RX synthesizers are locked to the same crystal to enable the desired coherent phase detection. The transmitter upconverts the IF signal to a 144GHz double-sideband signal (DSB) and broadcasts it to the target via a 5-stage caterpillar (named for its layout shape) PA with on-chip antenna. The on-chip antenna is formed by simply adding lifted (floating) bondwires onto the output pads forming a crude dipole antenna. The antenna gain is not high (<-10dBi) but sufficient to fulfill the radar's SNR requirements. At the receiver the 144GHz signal reflected back from the target is amplified by a 5-stage caterpillar LNA and downconverted. As the IF is quite low versus the carrier frequency, the narrow bandwidth associated with a 5-stage amplifier is still enough to support the DSB signal.

The phase estimation chip contains a delay-locked loop (DLL) with a D-flip-flop phase detector and a current-steering charge pump. The DLL chip copies the IF signal at the input of the TX and then tracks the phase of the received signal. This renders the DLL's control voltage proportional to the round-trip distance. The phase estimation chip can easily be integrated with the RX or TX chip but was separated in this work for testing purposes. Both LNA and PA are laid out as caterpillar amplifiers (based on transformer-coupled stages). The LNA uses cascode stages, while the PA uses common-source stages as the TX gain required is lower. At each stage the bias for the amplification and cascode devices is set by a control DAC. Control DACs are also used to adjust the bias of the frequency tripler, the VCO tuning, and the divider current control in the mm-Wave synthesizer. The schematic for the caterpillar LNA, the PA and their key performance metrics are shown in Fig 15.7.2.

Figure 15.7. 3 shows the test setup of the proposed radar indicating the location of TX, RX and the associated mm-Wave focusing lenses. Bistatic lenses are used for proof of concept, but a beamsplitter may be added in future systems to simplify the optics. The IF is provided externally using bench equipment. Using the setup shown in Fig.15.7.3, the distance response, INL (<0.76cm), and DNL (<0.15cm) were measured with an external 8-bit ADC and shown in Fig. 15.7.4. The definition of target distance vs. a 1m reference plane is also indicated.

In order to demonstrate the 3D imaging capability of the proposed sub-carrier SAR radar, a replica handgun and a roll of tape are imaged using a mechanical scanning stage placed in front of the radar. As shown in Fig. 15.7.5 the high 144GHz carrier provides excellent spatial/depth resolution (~3.3cm^2/0.76cm) capturing the details of both the gun and tape at over 1m of target distance.

The system performance data of the proposed radar is listed in Fig. 15.7.6 and compared against other state-of-the-art mm-Wave radar systems. The proposed sub-carrier SAR phased-based radar demonstrates 50X better depth resolution than that of the best FMCW CMOS radar at 77GHz [1] and 3X better than that of the best FMCW III-V radar [2]. It also shows 4X better in spatial resolution than that of CMOS references [1,3]. The total die area of the TX, RX and phase estimator chips is 4.38mm^2. Power consumption for the entire radar system is 457mW. Die photos of all thee chips are shown in Fig. 15.7.7 with major circuit blocks identified.

Acknowledgements:
Authors are grateful to TSMC for foundry support and P.H. Siegel from NASA Jet Propulsion Lab for several excellent technical discussions.

References:
[1] Yi-An Li, Meng-Hsiung Hung, Shih-Jou Huang, Jri Lee "A fully integrated 77GHz FMCW radar system in 65nm CMOS ", *ISSCC Dig. Tech. Papers*, pp. 216-217, Feb. 2010.
[2] Ken B. Cooper, Robert J. Dengler, Nuria Llombart, Tomas Bryllert,Goutam Chattopadhyay, Erich Schlecht, John Gill, Choonsup Lee, Anders Skalare, Imran Mehdi, and Peter H. Siegel, "Penetrating 3-D Imaging at 4 and 25m Range Using a Submillimeter-Wave Radar", *IEEE Trans. Microwave Theory and Techniques*, vol. 56, No. 12, pp. 2771-2778, Dec. 2008.
[3] Sakurai H, Kobayashi, Mitomo T, Watanabe O, Otaka S, "A 1.5GHz-modulation-range 10ms modulation-period 180kHz$_{rms}$-frequency-error 26MHz-reference mixed-mode FMCW synthesizer for mm-Wave radar application", *ISSCC Dig. Tech. Papers,* pp. 292-294, Feb. 2011.
[4] Sai-Wang Tam, Socher E, Wong, A, Yu Wang, Lan Duy Vu, Chang, M.-C.F., "Simultaneous sub-harmonic injection-locked mm-wave frequency generators for multi-band communications in CMOS", *IEEE Radio frequency Integrated Circuits Symp.*, pp. 131-134, June 2008.
[5] D. Murphy, Q.J. Gu, Yi-Cheng Wu, Heng-Yu Jian, Zhiwei Xu, A. Tang, A, F. Wang, M-C.F. Chang, "A Low Phase Noise, Wideband and Compact CMOS PLL for Use in a Heterodyne 802.15.3c Transceiver", *IEEE J. Solid-State Circuits*, vol. 46, No. 7, July 2011.

 978-1-4673-0377-4/12/$31.00

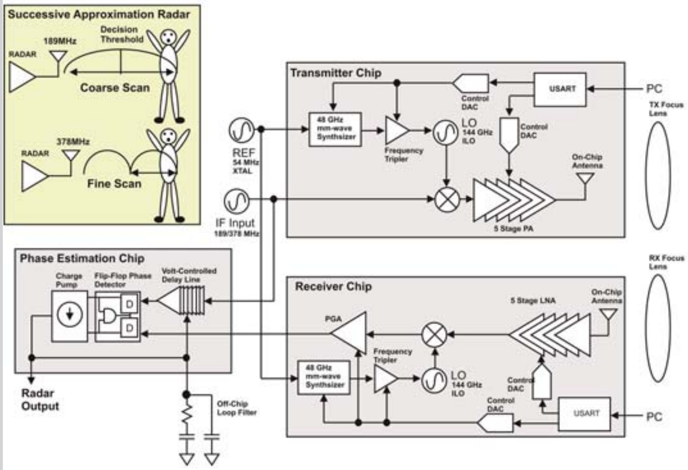

Figure 15.7.1: Principle of operation and block diagram of proposed sub-carrier SAR phase radar.

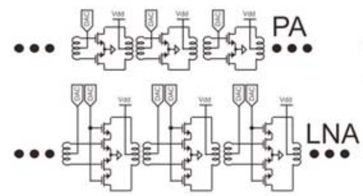

Transmitter Performance	
Saturated Output Power	10.1 dBm
TX Gain	9.7 dB
TX Output P1dB	7.3 dBm
TX 3dB Bandwidth	3.3 GHz
Receiver Performance	
RX Noise Figure	12.5 dB
RX Gain	48 dB
RX 3dB Bandwidth	1.7 GHz
144 GHz ILO Summary	
Phase Noise	-85 dBc / Hz @ 1 MHz**

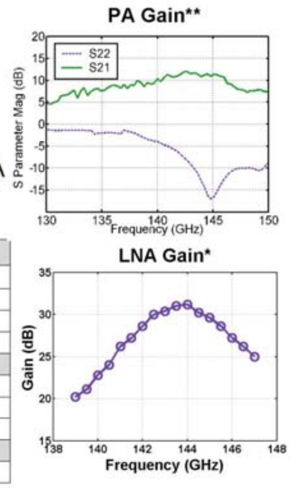

Figure 15.7.2: Schematics and performance of TX and RX mm-Wave front-end. *LNA gain is simulated values as stand-alone LNA is not available. ** PA and ILO are measured from stand-alone test chips.

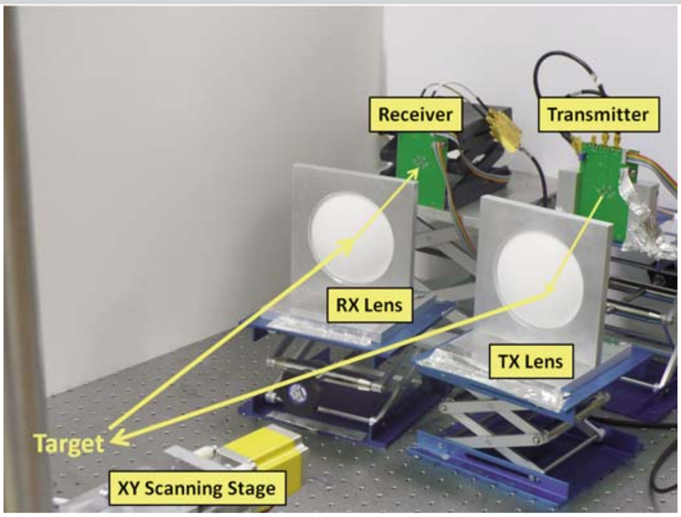

Figure 15.7.3: Test setup photo showing scanning stage and front-end bistatic optics. (note the lenses have been lowered so that TX and RX are visible in the picture.)

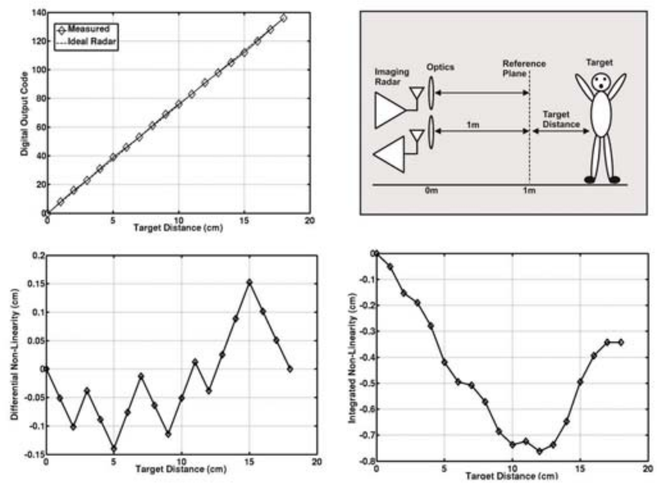

Figure 15.7.4: Target distance response, INL, DNL and spectrum of proposed sub-carrier SAR phase radar. Note the 0.0cm reference plane is set at 1m distance from the radar lenses. The scanning stage is limited to 18cm of travel in Z direction.

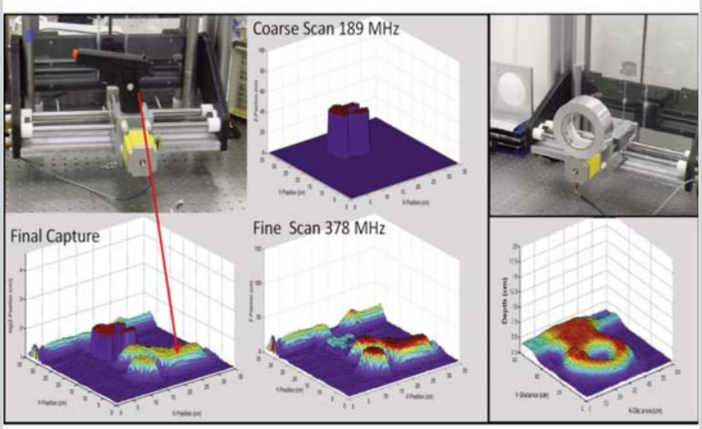

Figure 15.7.5: 3D Image capture showing coarse and fine capture steps of a replica handgun and metallic tape roll at 1m target distance with 2μs integration time. (Z-axis scaling has been adjusted to emphasize the 3D shapes.)

Transmitter Summary	
Saturated Output Power	10.1 dBm
Power Dissipation	219 mW
Die Area	1.82 mm²
Receiver Summary	
Power Dissipation	214 mW
Die Area	2.08 mm²
Noise Figure	12.5 dB
Phase Estimator Summary	
Power Dissipation	24mW
Die Area	0.48 mm²
System Performance	
XY Pixel Size at target (Spatial Res)	3.3 cm² with 14cm Lens at 1m target distance
Depth Resolution	0.76 cm (with 2us integration time)
Maximum Range	2.0 m (with a -20dB reflection coefficeint)

Radar Characteristic	[1]	[2]	[3]	This Work
Radar Type	FMCW	FMCW	FMCW	Sub-Carrier SAR (Phase)
XY Pixel Size at target	11.5 cm² @ 1m*	0.2cm² @ 1m*	11.5 cm²@ 1m*	3.3 cm² @ 1m
Depth Resolution	50cm	3.0 cm	N/A	0.76 cm (2us integration)
Power Dissipation (mW/pixel)	243mW	>10W	N/A	457mW
Total Area	1.05 mm²	Discrete	N/A	4.38 mm²
Frequency	77 GHz	600 GHz	77 GHz	144 GHz
Technology	65nm CMOS	III-V HBT	65nm CMOS	65nm CMOS

*scaled for using a 14cm lens diamater

Figure 15.7.6: Performance summary and comparison with state-of-the-art mm-Wave radars.

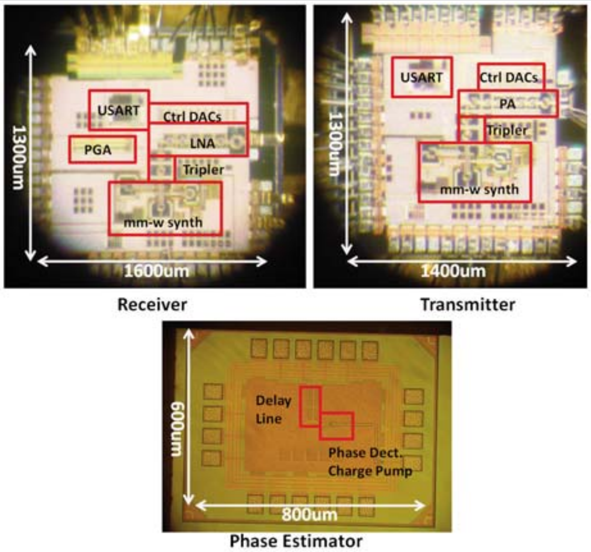

Figure 15.7.7: Die-photos of transmitter, receiver, and DLL chips.